International Journal of Chemical, Materials and Biomolecular Sciences
ISSN: 2415-6620
Vol:14, No:2, 2020

ROSA/LSTF Test on Pressurized Water Reactor Steam Generator Tube Rupture Accident Induced by Main Steam Line Break with Recovery Actions

Takeshi Takeda

***Abstract*—**An experiment was performed for the OECD/NEA ROSA-2 Project employing the ROSA/LSTF (rig of safety assessment/large-scale test facility), which simulated a steam generator tube rupture (SGTR) accident induced by main steam line break (MSLB) with operator recovery actions in a pressurized water reactor (PWR). The primary pressure decreased to the pressure level nearly-equal to the intact steam generator (SG) secondary-side pressure even with coolant injection from the high-pressure injection (HPI) system of emergency core cooling system (ECCS) into cold legs. Multi-dimensional coolant behavior appeared such as thermal stratification in both hot and cold legs in intact loop. The RELAP5/MOD3.3 code indicated the insufficient predictions of the primary pressure, the SGTR break flow rate, and the HPI flow rate, and failed to predict the fluid temperatures in the intact loop hot and cold legs. Results obtained from the comparison among three LSTF SGTR-related tests clarified that the thermal stratification occurs in the horizontal legs by different mechanisms.

***Keywords*—**LSTF, SGTR, thermal stratification, RELAP5.

I. Introduction

MSLB causes a fast depressurization of broken SG in a PWR, which results in the inflow of highly subcooled coolant into the core by considerably enhanced natural circulation in broken loop. In intact loop(s), flow stagnation may happen with thermal stratification in both hot and cold legs, especially after coolant is injected from ECCS. Following the MSLB, coolant for SG primary-side may be discharged to the secondary-side once SGTR happens on a U-tube in broken SG because of a significant increase in the pressure difference between the primary and secondary systems. If the SG main steam isolation valve is not properly closed in the MSLB case, a large amount of radionuclides would be directly released to the atmosphere through the broken SG main steam pipe.

There have been many of databases concerning either SGTR accident or MSLB of PWR by utilizing such integral test facilities as Semiscale [1], [2], LOFT (loss of fluid test) [3], LOBI (loop off-normal behavior investigations) [4], [5], BETHSY (boucle d'etudes thermohydraulique systeme) [6], IIST (institute of nuclear energy research integral system test) [7], PKL (primärkreisläufe versuchsanlage) [8], [9], and ATLAS (advanced thermal-hydraulic test loop for accident simulation) [10], [11]. An experiment designated as SB-SG-15 has been conducted with the ROSA/LSTF [12], simulating a PWR SGTR accident with operator interventions [13] for the OECD/NEA ROSA-2 Project [14]. Conditions of the SB-SG-15 test referred to those of the simulation test on the Mihama Unit-2 SGTR incident [15]. The LSTF simulates a Westinghouse-type four-loop 3,423 MW (thermal) PWR by a full-height and 1/48 volumetrically scaled two-loop system, and is 1/21 scale as compared to the two-loop Mihama Unit-2. The experimental and analytical studies, however, have been scarcely done for SGTR accident with MSLB [16], [17].

An LSTF experiment, denoted as SB-SG-14 for the OECD/NEA ROSA-2 Project, simulated a PWR SGTR accident induced by MSLB with operator recovery actions in 2010. Break size for MSLB was equivalent to 40% of 1/21 volumetrically scaled cross-sectional area of SG main steam tube in the two-loop Mihama Unit-2, considering the size of one SG flow restrictor. Break size for SGTR was for a double-ended guillotine break of the 1/21-scaled cross-sectional area of one of SG U-tubes in the two-loop Mihama Unit-2. When the primary pressure decreased to a certain pressure level, the HPI system of ECCS was started coolant injection into the cold legs at the full capacity. As illustrated in Fig. 1, the recovery actions involved the intact SG secondary-side depressurization by fully opening the SG relief valve (RV), the primary depressurization by fully opening a power-operated relief valve (PORV) in a pressurizer (PZR), and the throttle of flow rate of coolant injected from the HPI system into cold legs for the further primary depressurization. In the SB-SG-14 test, thermal stratification was observed in both hot and cold legs in intact loop in different ways (to be mentioned in Section IV *A*), which is important for the evaluation of pressurized thermal shock to the pressure vessel during the ECCS coolant injection [15], [18] in view of aging and plant life extension.

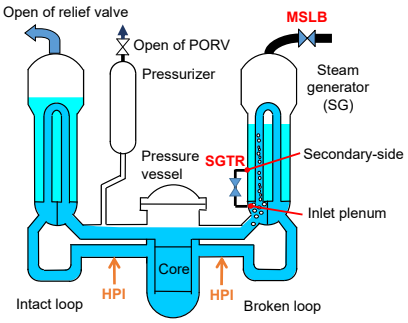

Fig. 1 Typical recovery actions in case of SGTR accident with MSLB

Takeshi Takeda is with Nuclear Regulation Authority, Roppongi, Minato-ku, Tokyo 106-8450, Japan (phone: 81-3-5114-2100; fax: 81-3-5114-2179; e-mail: takeda.takeshi4695@gmail.com).

In this study, the author analyzed the SB-SG-14 test by using RELAP5/MOD3.3 code [19] with more detailed model of the SGTR break unit than the model for which the posttest calculation has been performed with TRACE code [20], to assess the code predictive capability. Moreover, the author compared among the consequences of the SB-SG-14 test and those of two LSTF tests regarding the SGTR accident only. The two tests denoted as SB-SG-15 [13] and as SB-SG-10 [21] were carried out in 2010 and 1992, respectively. The objective of the comparison was to investigate effects of the MSLB and of the HPI coolant injection into the hot legs on the thermal stratification in the horizontal legs. In the SB-SG-15 test the SGTR break size was the same as that in the SB-SG-14 test, whereas it was equivalent to a double-ended guillotine break of the 1/48-scaled cross-sectional area of about six of SG U-tubes in the SB-SG-10 test. In the SB-SG-15 test the HPI coolant was injected into the cold legs similar to the SB-SG-14 test, whereas it was injected into not only the cold legs but the hot legs (like the combined injection of ECCS water in PWRs [22]) in the SB-SG-10 test. This paper presents major outcomes from the SB-SG-14 test and the RELAP5 code posttest analysis, and comparison among the three LSTF SGTR-related tests in terms of the thermal stratification in the horizontal legs.

II. ROSA/LSTF

The LSTF simulates a Westinghouse-type four-loop 3,423 MW (thermal) PWR by a two-loop system model with full-height and 1/48 in volume. The reference PWR of the LSTF is Tsuruga Unit-2. The schematic view of the LSTF is presented in Fig. 2. There are a pressure vessel, PZR, and primary loops in the LSTF. Each loop has an active SG, primary coolant pump, and hot and cold legs. Loops with and without PZR are designated as intact loop and broken loop, respectively. Each SG is equipped with 141 full-size U-tubes, inlet and outlet plena, boiler section, steam separator, steam dome, steam dryer, main steam line, four downcomer pipes, and other internals. The SG U-tube inner-diameter of 19.6 mm is the same as that in the reference PWR. The dimensions of hot and cold legs (inner-diameter of 207 mm each) are defined to conserve the volumetric scale (2/48) as well as the ratio of the length to the square root of the pipe diameter (Froude number basis) [23]. This is implemented to better simulate the flow regime transitions in the primary loops. The time scale of simulated thermal-hydraulic phenomena is one to one to that in the reference PWR. The LSTF core is 3.66 m in active height, which is composed of 1,008 electrically heated rods in 24 rod bundles as the simulated fuel rod assembly in the reference PWR. The axial profile of the LSTF core power is arranged in a nine-step chopped cosine in which a peaking factor is 1.495. The LSTF core power is limited to 10 MW that corresponds to 14% of the 1/48-scaled PWR nominal core power on account of a limitation in the capacity of power supply. The HPI system of ECCS has two plunger-type pumps with stroke adjustable flow control device; PJ (high-head charging) pump and PH (HPI) pump.

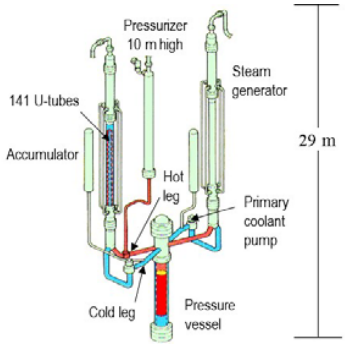

Fig. 2 Schematic view of ROSA/LSTF

III. LSTF Test and RELAP5 Code Analysis Conditions

A. SB-SG-14 Test Conditions

A 58.4 mm inner-diameter, sharp-edge orifice was mounted at the downstream of a pipe that was connected to the broken SG main steam line to model the MSLB. The SGTR was simulated by utilizing a 1.8 m-long nozzle with inner-diameter of 6.2 mm in the break unit in a piping that was connected between nozzles at inlet plenum and at secondary boiler section bottom of broken SG, as mentioned in Fig. 3.

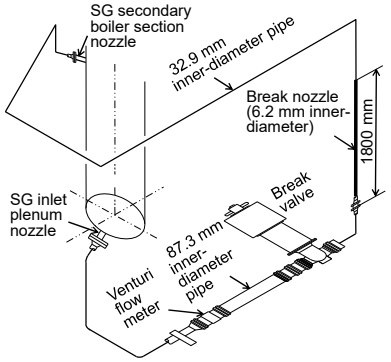

Fig. 3 Schematic view of SGTR break unit in SB-SG-14 test

Table I shows the major conditions of SB-SG-14 test. The experiment was launched by opening break valves installed for the SGTR and the MSLB concurrently at time zero. Initial steady-state conditions such as PZR pressure and fluid temperatures in the hot and cold legs were 15.5 MPa, 598 K, and 562 K, respectively, according to the reference PWR conditions. When the PZR pressure decreased to 12.97 MPa, a scram signal was obtained. Loss of off-site power was supposed to occur simultaneously with the scram signal, causing the closure of a SG main steam stop valve, the termination of SG main feedwater injection, and the coastdown of primary coolant pumps. The LSTF core power decay curve after the scram signal was predetermined by reference to some calculations making use of the RELAP5 code [24]. Initial SG secondary-side pressure was raised to 7.3 MPa to limit the primary-to-secondary heat transfer rate to 10 MW, which is higher than the nominal value of 6.1 MPa in the reference PWR. Initial SG secondary-side collapsed liquid level was

placed at 10.3 m which corresponds to the SG medium tube height. Setpoint pressure for opening and closure of SG RVs is 8.03 and 7.82 MPa respectively, referring to the setpoint value employed in the reference PWR.

TABLE I
MAJOR CONDITIONS OF SB-SG-14 TEST

Item	Condition
SGTR concurrent with MSLB	Time zero
Generation of scram signal	PZR pressure = 12.97 MPa
Generation of safety injection signal	Broken SG secondary-side pressure = 4.24 MPa
SG RV open/closure	SG secondary-side pressure = 8.03/7.82 MPa
Initiation of auxiliary feedwater injection into broken SG secondary-side	Generation of safety injection signal
Initiation of HPI coolant injection into cold legs at full capacity by PJ pump actuation	Primary pressure = 12.27 MPa
Initiation of intact SG RV full opening	30 min after safety injection signal
Initiation of auxiliary feedwater injection into intact SG secondary-side	Initiation of intact SG RV full opening
Initiation of PZR PORV full opening	Primary pressure stagnation
Termination of PZR PORV full opening	PZR liquid level = 1 m
Reduction of HPI flow rate to half capacity into cold legs switching over from PJ to PH pumps	Termination of PZR PORV full opening
Termination of auxiliary feedwater injection into broken SG secondary-side	Broken SG secondary-side collapsed liquid level = initial liquid level

When the broken SG secondary-side pressure reduced to 4.24 MPa, a safety injection signal was generated, which caused the initiation of auxiliary feedwater injection into the broken SG secondary-side. As a recovery action, the intact SG secondary-side depressurization was initiated by fully opening the SG RV 30 min after the safety injection signal, taking account of an international common understanding on a grace period to start an operator action [25]. Auxiliary feedwater was injected into the intact SG secondary-side concurrently with the recovery action. The intact SG RV full opening with the auxiliary feedwater injection into the intact SG secondary-side was continued thereafter. When the primary pressure decreased to 12.27 MPa, the HPI system was initiated coolant injection into the cold legs at the full capacity of employing the PJ pump. As another recovery action, the PZR PORV full opening was started when the primary pressure stagnated, and was terminated when the PZR liquid level reached 1 m. After the termination of the PZR PORV full opening, the HPI flow rate was reduced to the half capacity into the cold legs switching over from the PJ to PH pumps for the enhanced primary depressurization. When the broken SG secondary-side collapsed liquid level achieved the initial liquid level of 10.3 m, auxiliary feedwater injection into the broken SG secondary-side was terminated. The temperature of the auxiliary feedwater and the HPI coolant was 310 K, which is the same as that in the reference PWR. The flow rate of the auxiliary feedwater into each SG secondary-side was at a constant value of 0.6 kg/s. The actuation of the accumulator system of ECCS was suppressed to keep primary coolant discharge to SG secondary-side as low as possible.

B. RELAP5 Calculation Conditions of SB-SG-14 Test

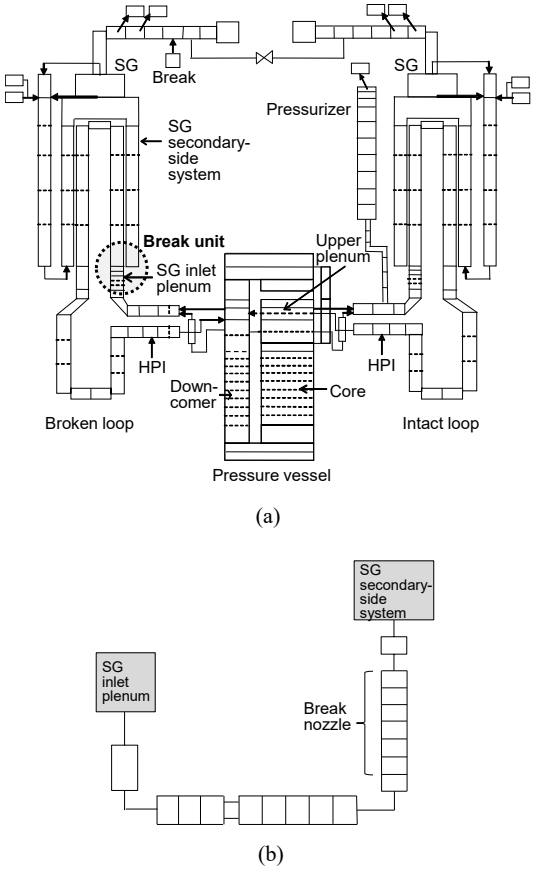

Fig. 4 (a) Overall schematic of LSTF system and (b) details of LSTF break unit for SGTR as noding schematic for RELAP5 code posttest analysis of SB-SG-14 test

As shown in Fig. 4 (a), one-dimensional manner of the LSTF system involved a pressure vessel, primary loops, PZR, SGs, and SG secondary-side system. As seen from Fig. 4 (b), the SGTR break unit in the piping connected between the inlet plenum and secondary-side system of broken SG (Fig. 3) was simulated by several vertical and horizontal pipes, taking the corresponding facility configuration into consideration. A long nozzle for the SGTR break was split into six equal-volume nodes. The posttest calculation employed a critical flow model that has been developed [26] with a discharge coefficient of 1.0, which may be fit to the simulation of a critical flow through a converging-diverging nozzle. The broken SG main steam line modeled was connected to one volume for simulating the MSLB, while a discharge coefficient of 0.84 was used only for single-phase discharge steam [27]. The core was divided into nine equal-height volumes that are vertically stacked according to nine-step chopped cosine power profile along the length of the core. The U-tubes in each SG were modeled by a single flow channel with nine nodes for the SG medium tube because the SG U-tubes were mostly full of liquid in the SB-SG-14 test. The HPI coolant injection was shortly stopped by switching over from the PJ to PH pumps in the SB-SG-14 test, whereas the successive HPI coolant injection was assumed in the

calculation. Other initial and boundary conditions were determined to be consistent with the SB-SG-14 test conditions.

IV. LSTF Test and RELAP5 Code Analysis Results

A. Major Phenomena Specific to SB-SG-14 Test

Table II shows the measurement uncertainty of typical parameter for identifying the major phenomena peculiar to the SB-SG-14 test, as submitted in Figs. 5-14. The measurement uncertainty is evaluated on the basis of the accuracy of the relevant instrument [12]. Suitable measurement precision of the typical parameter proved that the consistency of the measured data was ensured. Break flow rate through the break nozzle for the SGTR is measured by a venturi flow meter installed in the break unit (Fig. 3). The SGTR break flow rate took the peak just after the break (Fig. 5). Table III summarizes the chronology of the recovery actions during the time period of 0-5,000 s in the SB-SG-14 test. The primary pressure decreased simultaneously with the break, and reduced almost to the intact SG secondary-side pressure even with the coolant injection from the HPI system on account of the significant cooling effect by the MSLB (Fig. 6). By contrast, the intact SG secondary-side pressure rapidly increased up to 8 MPa after the closure of the SG main steam stop valve following the scram signal (Fig. 6). The SGTR break flow rate increased and stayed almost at a certain flow rate until the reduction of the HPI flow rate to the half capacity after the initiation of the HPI coolant injection (Figs. 5 and 7). After the start of the intact SG RV full opening, the primary pressure decreased a little and stagnated again. The PZR liquid level monotonically dropped after the break, and thus the PZR became empty of liquid (Fig. 8). The PZR PORV full opening brought about the primary depressurization and the quick recovery of the PZR liquid level. A gradual decrease appeared in the primary pressure during the time period in which the HPI flow rate was reduced from the full to half capacity. When the SGTR break flow rate reduced to equal to half capacity of the HPI flow rate, the primary pressure attained another pressure stagnation point.

TABLE II
Measurement Uncertainty of Typical Parameter in SB-SG-14 Test

Parameter	Uncertainty
SGTR break flow rate	±0.14 kg/s
PZR pressure	±0.108 MPa
SG secondary-side pressure	±0.054 MPa
HPI coolant injection flow rate	±0.02-0.05 kg/s
PZR liquid level	±0.25 m
SG secondary-side collapsed liquid level	±0.38 m
Primary loop flow rate	±1.25 kg/s
Hot leg fluid temperature	±2.75 K
Cold leg fluid temperature	±2.75 K

The broken SG secondary-side collapsed liquid level greatly decreased just after the MSLB, and gradually recovered after around 800 s by the auxiliary feedwater injection into the broken SG secondary-side (Fig. 9). A gradual increase continued in the broken SG secondary-side collapsed liquid level even after the termination of the auxiliary feedwater injection into the broken SG secondary-side. By contrast, the intact SG secondary-side collapsed liquid level was maintained constant at around 11 m until the start of the intact SG RV full opening. A great decrease began in the intact SG secondary-side collapsed liquid level thereafter. After around 2,800 s, a gradual recovery continued in the intact SG secondary-side collapsed liquid level because of the auxiliary feedwater injection into the intact SG secondary-side.

TABLE III
Chronology of Recovery Actions in SB-SG-14 Test

Event (0 to 5,000 s)	Time (s)
Initiation of HPI coolant injection into cold legs at full capacity by PJ pump actuation	147
Stop of primary coolant pumps	300
Initiation of intact SG RV full opening	1,853
Initiation of PZR PORV full opening	3,052
Termination of PZR PORV full opening	3,080
Termination of HPI coolant injection into cold legs at full capacity	3,100
Reduction of HPI flow rate to half capacity into cold legs by PH pump actuation	3,130

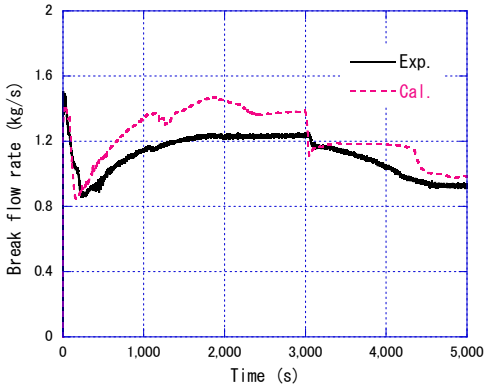

Fig. 5 SB-SG-14 test and calculated results for SGTR break flow rate

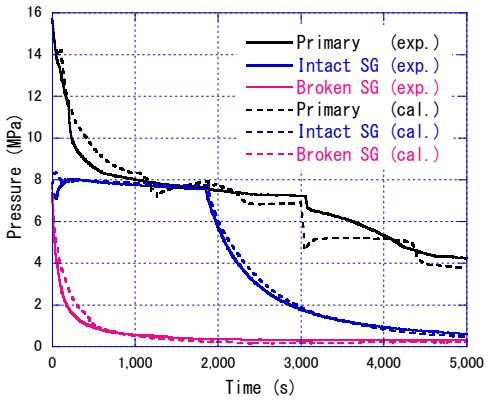

Fig. 6 SB-SG-14 test and calculated results for primary and SG secondary-side pressures in each loop

The primary loop flow rate is measured by utilizing a venturi flow meter at each primary coolant pump suction leg. Natural circulation began at around 300 s when the primary coolant pumps stopped (Fig. 10). Flow stagnation occurred in intact loop after around 1,000 s. The circulation flow rate was not

resumed in intact loop even after the start of the intact SG RV full opening. On the other hand, natural circulation prevailed in broken loop significantly. This caused that the core was filled with subcooled liquid, thereby leading to no core heatup.

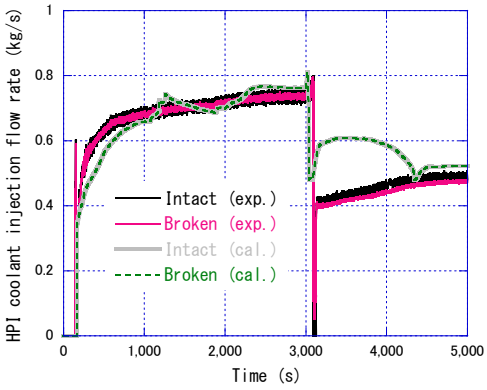

Fig. 7 SB-SG-14 test and calculated results for HPI coolant injection flow rate in each loop

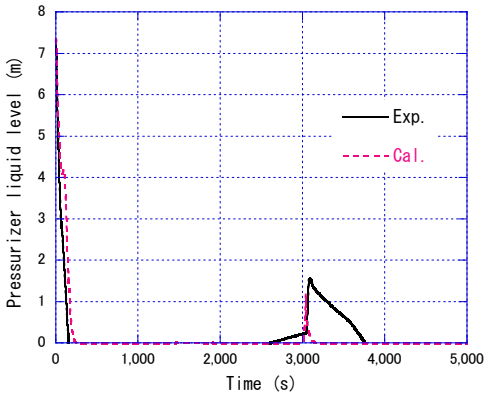

Fig. 8 SB-SG-14 test and calculated results for PZR liquid level

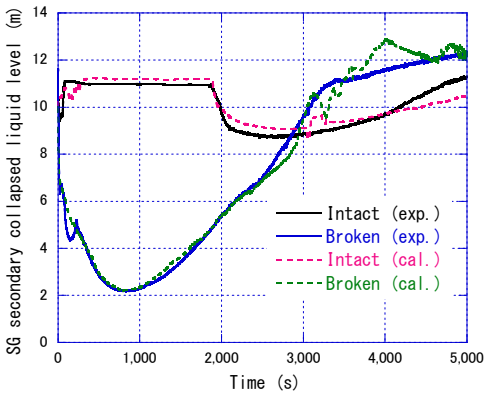

Fig. 9 SB-SG-14 test and calculated results for SG secondary-side collapsed liquid level in each loop

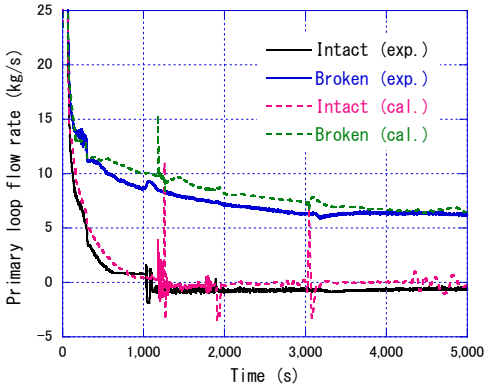

Fig. 10 SB-SG-14 test and calculated results for primary loop flow rate in each loop

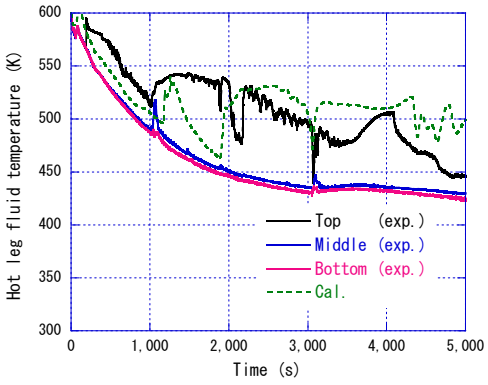

Fig. 11 SB-SG-14 test and calculated results for hot leg fluid temperature in intact loop

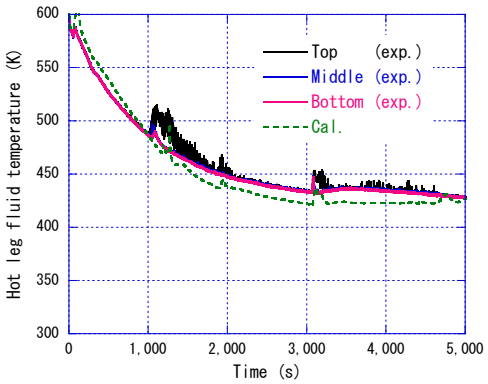

Fig. 12 SB-SG-14 test and calculated results for hot leg fluid temperature in broken loop

Fluid temperatures typically at the top, center, and bottom of the hot legs in intact loop and broken loop respectively are shown in Figs. 11 and 12, while those of the cold legs in intact loop and broken loop are indicated in Figs. 13 and 14. A temporal drop appeared in the hot leg liquid level in intact loop due to steam ingress from the PZR into the intact loop hot leg. By contrast, the hot leg in broken loop as well as the cold legs in both loops was full of liquid. Coolant in the hot leg was kept

subcooled, except the time period when the liquid level formed at the hot leg in intact loop. Thermal stratification took place in the intact loop hot leg where cold water layer occupied in around the bottom half region with uniform coolant temperature equal to that in the upper plenum, especially after the circulation flow rate became zero in intact loop (Fig. 11). Cold water migrated to the bottom of the hot leg from the upper plenum. Large fluid temperature fluctuated at the top portion of the hot leg. By contrast, the hot leg fluid temperatures were almost uniform in broken loop owing to adequate coolant mixing (Fig. 12). The cold leg fluid temperatures indicated subcooling. Cold water in the HPI system entered from the top of the cold legs, which caused thermal stratification in intact loop (Fig. 13). The range from the highest to lowest fluid temperatures expanded in the intact loop cold leg at around 1,000 s when the circulation flow rate became zero in intact loop. When the HPI flow rate was reduced to the half capacity, vertical fluid temperature profile shifted to higher temperature. By contrast, fluid temperature in the broken loop cold leg was almost uniform due to sufficient coolant mixing by significant natural circulation arisen from the MSLB (Fig. 14).

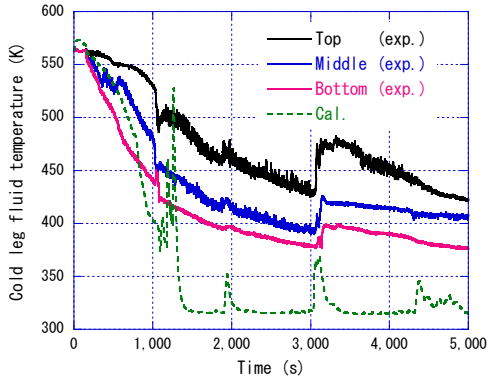

Fig. 13 SB-SG-14 test and calculated results for cold leg fluid temperature in intact loop

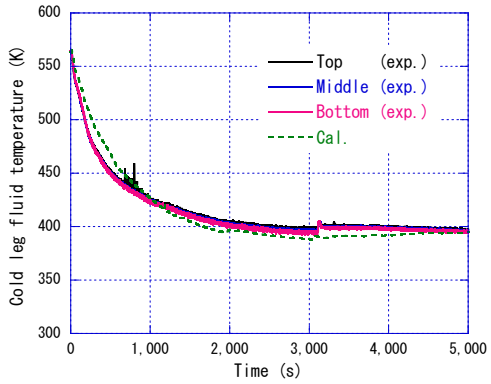

Fig. 14 SB-SG-14 test and calculated results for cold leg fluid temperature in broken loop

B. Assessment of RELAP5 Code Predictive Capability

The RELAP5 code predicted the overall trends of the major thermal-hydraulic responses observed in the SB-SG-14 test well, as presented in Figs. 5-14. Until around 1,300 s, the primary pressure was overpredicted due to the overprediction of the broken SG secondary-side pressure, thereby giving rise to the overestimation of the SGTR break flow rate and the underestimation of the HPI flow rate (Figs. 5-7). The primary pressure was temporarily lower than the intact SG secondary-side pressure in the calculation only. This led to the decrease in the calculated SGTR break flow rate and the larger increase in the HPI flow rate in the calculation compared to the experiment. The code predicted the decrease in the intact SG secondary-side pressure after the intact SG RV full opening. However, the decreasing rate of the primary pressure was larger in the calculation than in the experiment. This caused the decrease in the calculated SGTR break flow rate and the larger increase in the HPI flow rate in the calculation compared to the experiment. The code roughly reproduced the primary pressure stagnation, though with a tendency that the primary pressure was underpredicted. After the start of the PZR PORV full opening, the primary pressure was underpredicted, which resulted in the underestimation of the SGTR break flow rate and the overestimation of the HPI flow rate. After the termination of the PZR PORV full opening, the PZR became empty of liquid in a shorter time in the calculation than in the experiment (Fig. 8). After the reduction of the HPI flow rate to the half capacity, the primary pressure stayed almost at a certain pressure level in the calculation only. This gave rise to no substantial changes in the calculated SGTR break flow rate and the calculated HPI flow rate. A large decrease appeared in the primary pressure after around 4,300 s in the calculation only, which resulted in substantial decreases in the calculated SGTR break flow rate and the calculated HPI flow rate. The calculated secondary-side collapsed liquid levels of both SGs agreed reasonably well with the measured liquid levels (Fig. 9).

The code roughly reproduced the asymmetric natural circulation between two loops, though with a tendency that the circulation flow rate was a little overpredicted with some oscillation (Fig. 10). The calculated cross-sectional average fluid temperatures in the broken loop hot and cold legs were in reasonably well agreement with the measured fluid temperatures (Figs. 12 and 14). The code revealed a difficulty in correctly dealing with thermal stratification in the intact loop hot and cold legs due to the one-dimensional representation (Figs. 11 and 13). The intact loop hot leg fluid cross-sectional average temperature obtained from the calculation became higher than the hot leg fluid temperature obtained experimentally after around 2,000 s. The calculated cross-sectional average fluid temperature in the intact loop cold leg became much lower than the measured fluid temperature after around 1,300 s. This may be attributed to the overestimation of the cooling effect by the HPI water. The combined use with three-dimensional computational fluid dynamics code [28] may thus be needed for better prediction of multi-dimensional coolant behavior in the horizontal legs.

V. Thermal Stratification in Horizontal Legs

A. Comparison of Two SGTR-Related Tests with or without MSLB

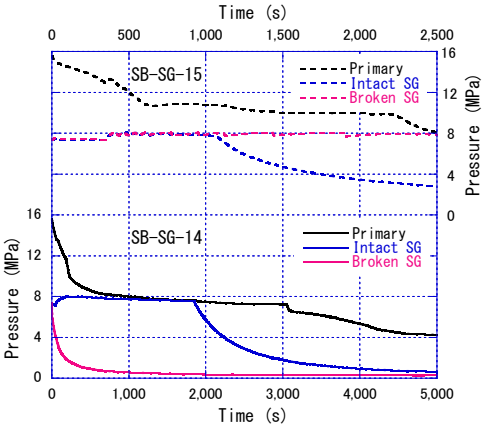

Fig. 15 SB-SG-14 and SB-SG-15 test results for primary and SG secondary-side pressures in each loop

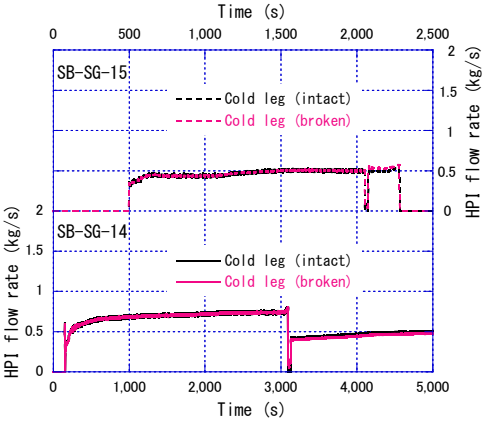

Fig. 16 SB-SG-14 and SB-SG-15 test results for HPI coolant injection flow rate in each loop

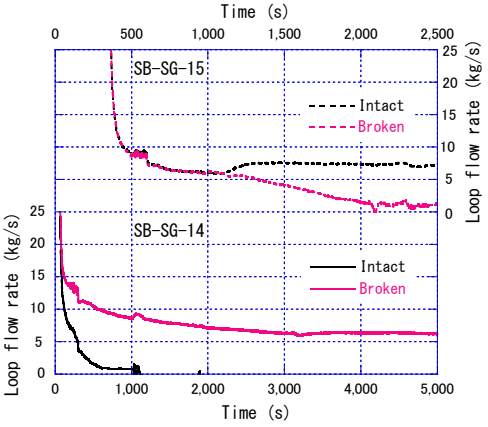

Fig. 17 SB-SG-14 and SB-SG-15 test results for primary loop flow rate in each loop

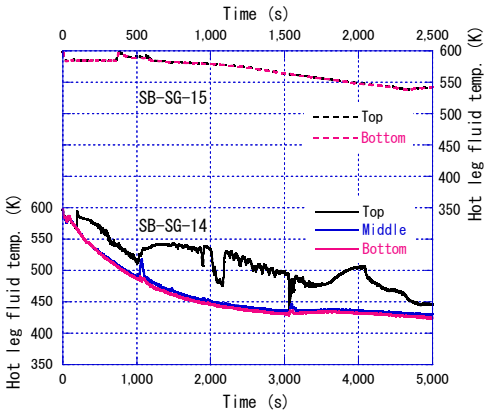

Fig. 18 SB-SG-14 and SB-SG-15 test results for hot leg fluid temperature in intact loop

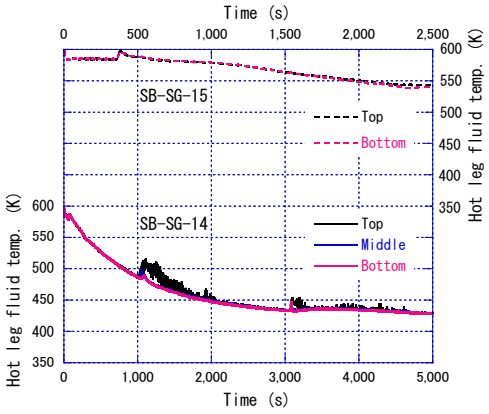

Fig. 19 SB-SG-14 and SB-SG-15 test results for hot leg fluid temperature in broken loop

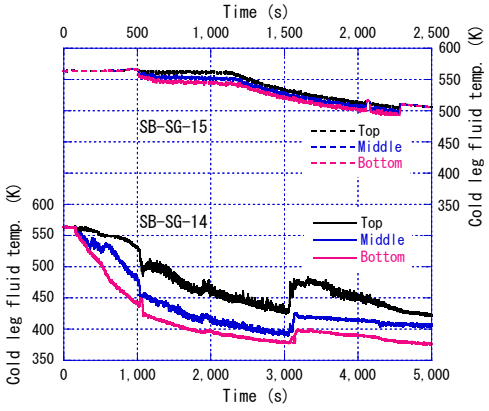

Fig. 20 SB-SG-14 and SB-SG-15 test results for cold leg fluid temperature in intact loop

Results of the SB-SG-14 test were compared with those of the SB-SG-15 test to clarify influences of the MSLB on the thermal stratification in the horizontal legs, as shown in Figs. 15-21. The common condition of the SB-SG-14 and SB-SG-15 tests was the HPI coolant injection into the cold legs. However,

the HPI flow rate remained unchanged at the full capacity in the SB-SG-15 test, in contrast to the SB-SG-14 test. Table IV shows the chronology of the recovery actions such as the intact SG RV full opening, the PZR auxiliary spray, and the HPI coolant injection into the cold legs during the time period from 0 to 2,500 s in the SB-SG-15 test. The following are major results from the SB-SG-15 test.

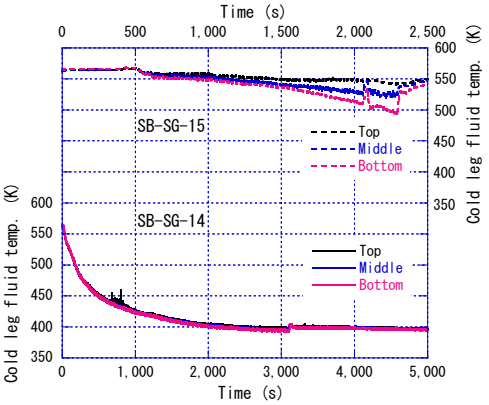

Fig. 21 SB-SG-14 and SB-SG-15 test results for cold leg fluid temperature in broken loop

TABLE IV
CHRONOLOGY OF RECOVERY ACTIONS IN SB-SG-15 TEST

Event (0 to 2,500 s)	Time (s)
Initiation of HPI coolant injection into cold legs by PJ pump actuation	497
Stop of primary coolant pumps	602
Initiation of intact SG RV full opening	1,076
Termination of HPI coolant injection into cold legs	2,055
Initiation of HPI coolant injection into cold legs by PH pump actuation	2,075
Initiation of PZR auxiliary spray	2,110
Termination of HPI coolant injection into cold legs	2,283

The primary pressure was held higher than the broken SG secondary-side pressure because of the HPI coolant injection into the cold legs (Figs. 15 and 16). The primary pressure was intentionally lowered to the broken SG secondary-side pressure through the PZR auxiliary spray with the termination of the HPI coolant injection. Significant natural circulation was dominant in intact loop after the start of the intact SG RV full opening, while the circulation flow rate became close to zero in broken loop especially after the initiation of the PZR auxiliary spray (Fig. 17). The hot leg fluid temperatures in both loops were almost uniform until the pressure equalization was achieved between the primary and broken SG secondary sides after the break (Figs. 18 and 19). Thermal stratification was seen in the cold legs in both loops during the HPI coolant injection. The fluid temperature at the cold leg bottom was lower than that at the cold leg top in intact loop (Fig. 20). After the start of the SG RV full opening, however, the degree of thermal stratification decreased due to the significant natural circulation. Cold water was highly stagnated at the cold leg bottom in broken loop owing to the low circulation flow rate (Fig. 21). The difference in the broken loop cold leg fluid temperature between the top and bottom increased with decreasing the circulation flow rate after the start of the intact SG RV full opening. The circulation flow rates in individual loops were quite different between the two SGTR-related tests with or without the MSLB. Comparison results of the SB-SG-14 and SB-SG-15 tests revealed that the thermal stratification in the cold legs in both loops largely depends on the combination of the HPI coolant injection into the cold legs and the circulation flow rate.

B. Comparison of Two SGTR-Related Tests with or without HPI Coolant Injection into Hot Legs

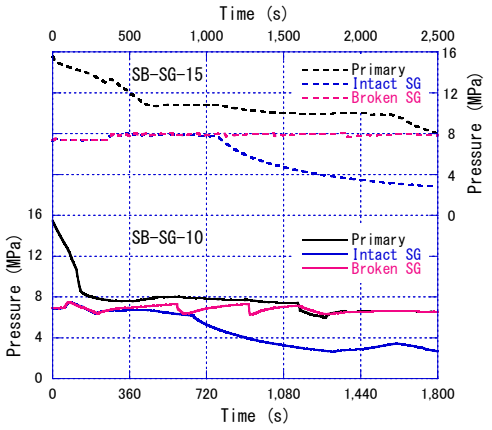

Fig. 22 SB-SG-10 and SB-SG-15 test results for primary and SG secondary-side pressures in each loop

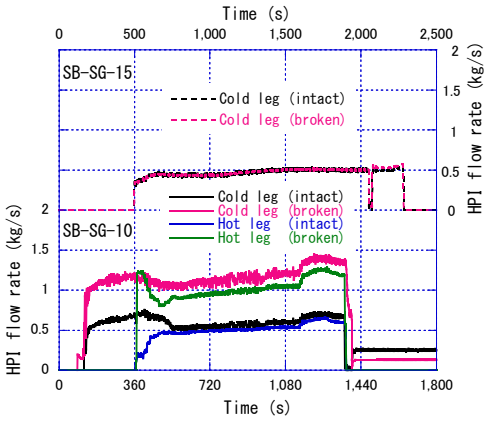

Fig. 23 SB-SG-10 and SB-SG-15 test results for HPI coolant injection flow rate in each loop

Results of the SB-SG-10 test were compared with those of the SB-SG-15 test to make clear influences of the HPI coolant injection into the hot legs on the thermal stratification in the horizontal legs, as indicated in Figs. 22-28. No fluid temperatures at the center of both the hot and cold legs are measured in the SB-SG-10 test. The SB-SG-10 and SB-SG-15 tests belonged to the SGTR accident only but with different break size. Table V indicates the chronology of the recovery actions including the intact SG RV full opening, the PZR PORV full opening, and the HPI coolant injection into both the hot and cold legs during the time period of 0-1,800 s in the

SB-SG-10 test. Major results from the SB-SG-10 test are described in the following.

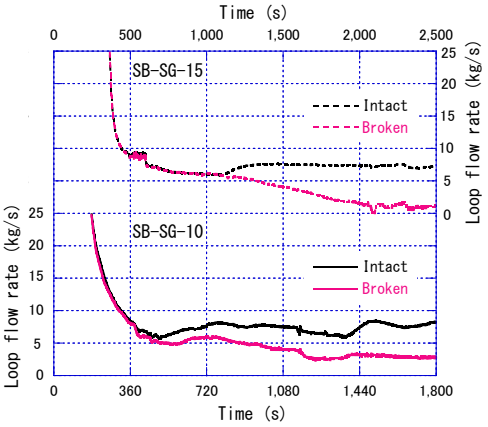

Fig. 24 SB-SG-10 and SB-SG-15 test results for primary loop flow rate in each loop

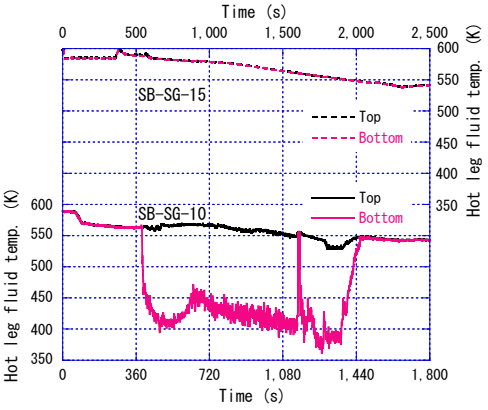

Fig. 25 SB-SG-10 and SB-SG-15 test results for hot leg fluid temperature in intact loop

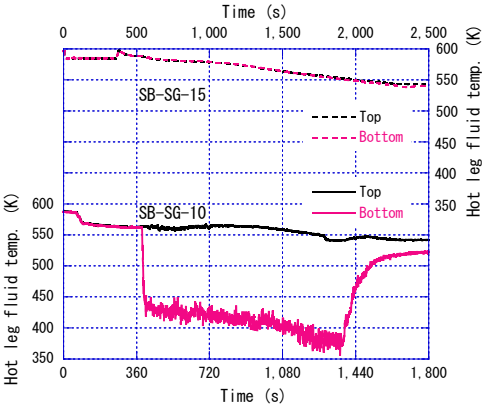

Fig. 26 SB-SG-10 and SB-SG-15 test results for hot leg fluid temperature in broken loop

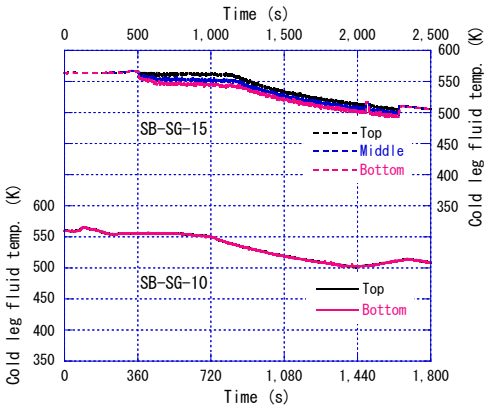

Fig. 27 SB-SG-10 and SB-SG-15 test results for cold leg fluid temperature in intact loop

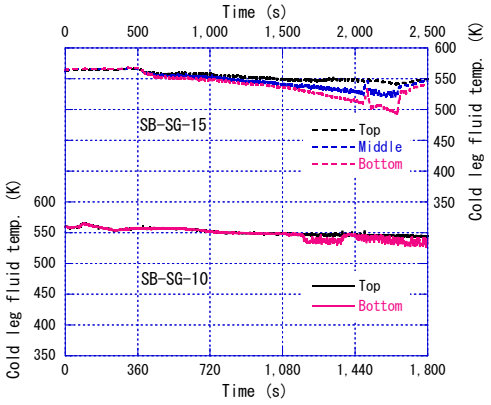

Fig. 28 SB-SG-10 and SB-SG-15 test results for cold leg fluid temperature in broken loop

TABLE V
CHRONOLOGY OF RECOVERY ACTIONS IN SB-SG-10 TEST

Event (0 to 1,800 s)	Time (s)
Initiation of HPI coolant injection into cold legs by PJ pump actuation	80
Initiation of HPI coolant injection into hot legs by PH pump actuation	370
Stop of primary coolant pumps	457
Initiation of intact SG RV full opening	655
Initiation of PZR PORV full opening	1,146
Termination of PZR PORV full opening	1,277
Termination of intact SG RV full opening	1,314
Termination of HPI coolant injection into cold legs	1,365
Termination of HPI coolant injection into hot legs	1,376
Initiation of HPI coolant injection into cold legs by PH pump actuation	1,400

The primary pressure was maintained higher than the broken SG secondary-side pressure during the HPI coolant injection into both the hot and cold legs even after the start of the intact SG RV full opening (Figs. 22 and 23). The PZR PORV full opening contributed to the pressure equalization between the primary and broken SG secondary sides. Natural circulation prevailed in intact loop significantly after the start of the intact SG RV full opening, while the circulation flow rate became

relatively-low in broken loop after the initiation of the PZR PORV full opening (Fig. 24). The fluid temperature at the hot leg bottom was considerably lower than that at the hot leg top in both loops during the HPI coolant injection into the hot legs (Figs. 25 and 26). The flow rate of the HPI coolant injected into the hot legs in both loops thus proved to be highly sensitive to the degree of thermal stratification in the hot legs. After the start of the intact SG RV full opening, the cold leg fluid temperatures were uniform in intact loop because of the significant natural circulation (Fig. 27). After the start of the PZR PORV full opening, on the other hand, the fluid temperature at the cold leg bottom was a little lower than that at the cold leg top in broken loop owing to the relatively-low circulation flow rate (Fig. 28). The natural circulation flow behavior led to adequate coolant mixing, which resulted in no thermal stratification in the cold legs in both loops. Comparison results of the SB-SG-10 and SB-SG-15 tests confirmed that the thermal stratification in the hot legs in both loops is largely affected by the HPI coolant injection into the hot legs.

VI. Summary

An LSTF experiment was conducted for the OECD/NEA ROSA-2 Project, simulating a PWR SGTR accident induced by MSLB with operator recovery actions. The recovery actions included the intact SG secondary-side depressurization by fully opening the SG RV, the primary depressurization by fully opening the PZR PORV, and the throttle of the HPI coolant flow rate injected into cold legs. The posttest analysis of the LSTF test was carried out by using the RELAP5/MOD3.3 code to evaluate the code predictive capability. Furthermore, results of three LSTF SGTR-related tests were compared focusing on effects of the MSLB and of the HPI coolant injection into the hot legs on thermal stratification in the horizontal legs. Major outcomes are summarized as follows.

In the LSTF test on the SGTR accident with MSLB, the primary pressure decreased almost to the intact SG secondary-side pressure on account of the significant cooling effect by the MSLB even with the HPI coolant injection. The intact SG RV full opening caused that the primary pressure decreased a little and stagnated again. The primary pressure gradually decreased after the reduction of the HPI flow rate to the half capacity, which led to another pressure stagnation point. Thermal stratification was seen in both hot and cold legs in intact loop due to the ingress of low-temperature coolant into the hot leg from the upper plenum and the stagnation of high-temperature coolant over the HPI coolant in the cold leg. On the other hand, no thermal stratification took place in the broken loop hot and cold legs owing to significant natural circulation arisen from the MSLB.

The RELAP5 code predicted the overall tendencies of the major thermal-hydraulic responses observed in the LSTF test well. The code also qualitatively reproduced the primary pressure stagnation and the asymmetric natural circulation between two loops. However, there were some differences in the primary pressure, the SGTR break flow rate, and the HPI flow rate between the LSTF test and the posttest calculation. The fluid temperatures in the intact loop hot and cold legs were not properly calculated owing to a difficulty in the prediction of multi-dimensional coolant behavior by the code with the one-dimensional representation.

In the LSTF test on the SGTR accident only with the HPI coolant injection into the cold legs, thermal stratification occurred in the broken loop cold leg because of the low circulation flow rate until the termination of the HPI coolant injection, while significant natural circulation lowered the degree of thermal stratification in the intact loop cold leg after the initiation of the intact SG RV full opening. In the LSTF test on the SGTR accident only with the HPI coolant injection into both the hot and cold legs, thermal stratification took place in the hot legs in both loops during the HPI coolant injection into the hot legs, and the degree of thermal stratification was largely dependent on the HPI flow rate.

Acknowledgment

The author would like to thank Messrs. M. Ogawa and A. Ohwada of Japan Atomic Energy Agency for performing the LSTF test under collaboration with members from Nuclear Engineering Co. as well as Miss K. Toyoda of Research Organization for Information Science and Technology for manipulating the experimental data.

References

[1] G.G. Loomis, “Steam generator tube rupture in an experimental facility scaled from a pressurized water reactor,” in: *Proc. of the 5th International Meeting on Thermal Nuclear Reactor Safety*, Karlsruhe, Germany, October 1984.

[2] J.M. Rogers, “An analysis of Semiscale Mod-2C S-FS-1 steam line break test using RELAP5/MOD2,” NUREG/IA-0052, USNRC, Washington, DC, 1992.

[3] G. Srikantiah, “Methods for PWR transient analysis,” Nucl. Eng. Des., vol. 83, 1984, pp. 189–198.

[4] G.F. De Santi, “Analysis of steam generator U-tube rupture and intentional depressurization in LOBI-MOD2 facility,” Nucl. Eng. Des., vol. 126, 1991. pp. 113–125.

[5] C. Addabbo and A. Annunziato, “The LOBI integral system test facility experimental programme,” Sci. Technol. Nucl. Installations, vol. 2012, 2012, Article 238019, pp. 1–16.

[6] J.C. Barbier, P. Clement, and R. Deruaz, “A single SGTR with unavailability of both the high pressure safety injection system and the steam generator auxiliary feedwater system on BETHSY integral test facility,” in: *Proc. of the International Conference on New Trends in Nuclear System Thermalhydrulics*, Pisa, Italy, May-June 1994.

[7] T.J. Liu, C.H. Lee, C.C. Yao, and S.C. Chiang, “An evaluation of emergency operator actions by an experimental SGTR event at the IIST facility and a comparison of Mihama-2 SGTR event record,” Nucl. Technol., vol. 129, 2000, pp. 36–50.

[8] K. Umminger, T. Mull, and B. Brand, “Integral effect tests in the PKL facility with international participation,” Nucl. Eng. Technol., vol. 41, 2009, pp. 765–774.

[9] K. Umminger, L. Dennhardt, S. Schollenberger, and B. Schoen, “Integral Test Facility PKL: Experimental PWR Accident Investigation,” Sci. Technol. Nucl. Installations, Article ID 891056, vol. 2012, 2012, pp. 1–16.

[10] K.Y. Choi, Y.S. Kim, C.H. Song, and W.P. Baek, “Major achievements and prospect of the ATLAS integral effect tests,” Sci. Technol. Nucl. Installations, vol. 2012, 2012, Article 375070, pp. 1–18.

[11] K.H. Kang, Y.S. Park, B.U. Bae, J.R. Kim, N.H. Choi, and K.Y. Choi, “Code assessment of ATLAS integral effect test simulating main steam-line break accident of an advanced pressurized water reactor,” J. Nucl. Sci. Technol., vol. 55, 2018, pp. 104–112.

[12] The ROSA-V Group, “ROSA-V Large Scale Test Facility (LSTF) System Description for the Third and Fourth Simulated Fuel Assemblies,” JAERI-Tech 2003-037, Japan Atomic Energy Research Institute, Ibaraki,

Japan, 2003.
[13] T. Takeda, "ROSA/LSTF test and RELAP5 code analyses on PWR steam generator tube rupture accident with recovery actions," Nucl. Eng. Technol., vol. 50, 2018, pp. 981–988.
[14] NEA, "Final Integration Report of Rig-of-safety Assessment (ROSA-2) Project - 2009–2012," NEA/CSNI/R(2016)10, 2017.
[15] T. Watanabe, "Effects of ECCS on the cold-leg fluid temperature during SGTR accidents," Int. J. Mech. Mechatronics Eng., vol. 9, 2015, pp. 1618–1622.
[16] G. Jimenez, C. Queral, M.J. Rebollo-Mena, J.C. Martínez-Murillo, and E. Lopez-Alonso, "Analysis of the operator action and the single failure criteria in a SGTR sequence using best estimate assumptions with TRACE 5.0," Ann. Nucl. Energy, vol. 58, 2013, pp. 161–177.
[17] K.Y. Choi, K.H. Kang, and C.H. Song, "Recent achievement and future prospects of the ATLAS program," Nucl. Eng. Des., vol. 354, 2019, Article 110168, pp. 1–10.
[18] D. Lucas, D. Bestion, E. Bodèle, et al., "An overview of the pressurized thermal shock issue in the context of the NURESIM Project," Sci. Technol. Nucl. Installations, vol. 2009, 2009, Article 583259, pp. 1–13.
[19] USNRC Nuclear Safety Analysis Division, "RELAP5/MOD3.3 Code Manual," NUREG/CR-5535/Rev 1, Information Systems Laboratories, Inc., 2001.
[20] S. Gallardo, A. Querol, M. Lorduy, and G. Verdu, "Assessment of TRACE 5.0 against ROSA-2 Test 5, Main Steam Line Break with Steam Generator Tube Rupture," NUREG/IA-0505, Rev. 1, USNRC, Washington, DC, 2019.
[21] K.W. Seul, Y.S. Bang, I.G. Kim, T. Yonomoto, and Y. Anoda, "Simulation of multiple steam generator tube rupture (SGTR) event scenario," J. Korean Nucl. Soc., vol. 35, 2003, pp. 179–190.
[22] E.F. Hicken, "Important thermohydraulic aspects during refilling and reflooding of an uncovered LWR core," in: *Proc. of a Seminar on the Results of the European Communities' Indirect Action Research Programme on Safety of Thermal Water Reactors*, Brussels, Belgium, October 1984.
[23] N. Zuber, "Problems in Modeling Small Break LOCA," NUREG-0724, USNRC, Washington, DC, 1980.
[24] H. Kumamaru and K. Tasaka, "Recalculation of Simulated Post-scram Core Power Decay Curve for Use in ROSA-IV/LSTF Experiments on PWR Small-break LOCAs and Transients," JAERI-M 90-142, Japan Atomic Energy Research Institute, Ibaraki, Japan, 1990.
[25] NEA, "Final Integration Report of OECD/NEA ROSA Project 2005–2009," NEA/CSNI/R(2013)1, 2013.
[26] V.H. Ransom and J.A. Trapp, "The RELAP5 choked flow model and application to a large scale flow test," in: *Proc. of the ANS/ASME/NRC International Topical Meeting on Nuclear Reactor Thermal-Hydraulics*, Saratoga Springs, New York, USA, October 1980.
[27] D.W. Sallet, "Thermal hydraulics of valves for nuclear applications," Nucl. Sci. Eng., vol. 88, 1984, pp. 220–244.
[28] NEA, "Best Practice Guidelines for the Use of CFD in Nuclear Reactor Safety Applications - Revision," NEA/CSNI/R(2014)11, 2015.

Takeshi Takeda is on loan to Nuclear Regulation Authority from Japan Atomic Energy Agency. His interests include thermal-hydraulic safety during accidents and abnormal transients of light water reactor through experiments using test facilities and by calculations with best-estimate computer code.